Neuron, Vol. 32, 1181–1192, December 20, 2001, Copyright ©2001 by Cell Press

Stability of Cortical Responses and the Statistics of Natural Scenes

Valentin Dragoi,[1] Camelia M. Turcu, and Mriganka Sur
Department of Brain and Cognitive Sciences
Massachusetts Institute of Technology
Cambridge, Massachusetts 02139

Summary

The primary visual cortex (V1) of higher mammals contains maps of stimulus features; how these maps influence vision remains unknown. We have examined the functional significance of an asymmetry in the orientation map in cat V1, i.e., the fact that a larger area of V1 is preferentially activated by vertical and horizontal contours than by contours at oblique orientations. Despite the fact that neurons tuned to cardinal and oblique orientations have indistinguishable tuning characteristics, cardinal neurons remain more stable in their response properties after selective perturbation induced by adaptation. Similarly, human observers report different adaptation-induced changes in orientation tuning between cardinal and oblique axes. We suggest that the larger cortical area devoted to cardinal orientations imposes stability on the processing of cardinal contours during visual perception, by retaining invariant cortical responses along cardinal axes.

Introduction

V1 of higher mammals contains two-dimensional representations, or maps, for different stimulus features superimposed on a continuous retinotopic map of visual space. The geometry of several kinds of maps in V1 such as those for stimulus orientation, spatial frequency, and ocular dominance (Hübener et al., 1997) have now been described in detail. And yet, the functional significance of cortical maps for neuronal processing and for visual perception remains unknown.

Orientation maps in V1, for instance, consist of neurons of similar orientation preference clustered together in domains that cover almost the entire cortical surface (Hubel and Wiesel, 1974; Bonhoeffer and Grinvald, 1991; Blasdel, 1992), with the exception of singularities such as pinwheel centers (Bonhoeffer and Grinvald, 1991; Blasdel, 1992) where all orientations converge. Computational models have suggested that orientation maps represent optimal structures that maximize coverage (Durbin and Mitchison, 1990; Swindale et al., 2000) or minimize the length of cortical wiring (Koulakov and Chlovskii, 2001). However, optimization principles cannot address whether the structure of orientation maps is functionally significant for vision. Thus, we have asked whether the size of orientation domains can constrain the integration of inputs by neurons in V1 of adult cats and then devised psychophysical experiments in human subjects to test physiological predictions.

One striking aspect of natural vision is the orientation statistics of contours in natural environments. Image analysis (Figure 1) reveals that the distribution of oriented contours is biased toward horizontal and vertical edges relative to the obliques (e.g., Switkes et al., 1978; Coppola et al., 1998a). This asymmetry raises the question of whether the distribution of orientation-selective neurons in the visual cortex is influenced by the prevalence of vertical and horizontal contours in natural scenes. Indeed, it has been demonstrated using single-cell recording (Pettigrew et al., 1968; Blakemore and Cooper, 1970; Albus, 1975; Leventhal and Hirsch, 1977; Stryker et al., 1978; Kennedy and Orban, 1979; De Valois et al., 1982; Levitt et al., 1994) and optical imaging of intrinsic signals (Chapman and Bonhoeffer, 1998; Coppola et al. 1998b; Müller et al., 2000) that the organization of orientation columns in adult ferret and cat V1 contains an overrepresentation of cardinal orientations (Figures 2A and 2B). The bias toward cardinal preferences has been reported to be more pronounced in ferret V1 than in cat V1 (Müller et al., 2000), although interanimal variability in the representation size has also been reported (Campbell et al., 1968; Rose and Blakemore, 1974; Blakemore and Van Sluyters, 1975). This overrepresentation could arise by innate specification (Coppola et al., 2000) and can be further amplified by exposure to anisotropic environments during development (Sengpiel et al., 1999). However, the functional significance of the representational anisotropy is unknown.

We reasoned that the overrepresentation of certain orientations in visual cortex could bias the orientation distribution of local inputs to cortical neurons based on the neuron's location in the map of orientation preference. We hypothesized that the basin of short-range intracortical inputs to a cortical neuron is restricted to the area surrounding the neuron's location in the orientation map and that the orientation specificity of local inputs is determined by the distribution of pixel orientations in this local area. Figure 2C, which represents the orientation distribution of representative circular patches obtained after imaging V1, shows that a larger cortical space devoted to cardinal orientations can constrain the distribution of oriented inputs within a local domain. Considering that local excitatory and inhibitory inputs to cortical cells originate in the immediate vicinity of the cell bodies from within $\sim$500 μm radius (Hata et al., 1991; Malach et al., 1993; Weliky et al., 1995; Kisvarday et al., 1997), we pooled all the pixels within the local circuit into eight orientation bins between 0° and 180°. We found that neurons situated in the middle of a cardinal orientation domain have a preponderence of iso-oriented inputs (Figure 2C), whereas neurons situated in the middle of an oblique orientation domain receive inputs from areas of larger orientation spread (Figure 2D). Thus, altering the efficacy of specific local inputs would change the response properties of neurons tuned to cardinal and oblique orientations to different extents. One way to alter the efficacy of intracortical inputs to a

[1] Correspondence: vdragoi@ai.mit.edu

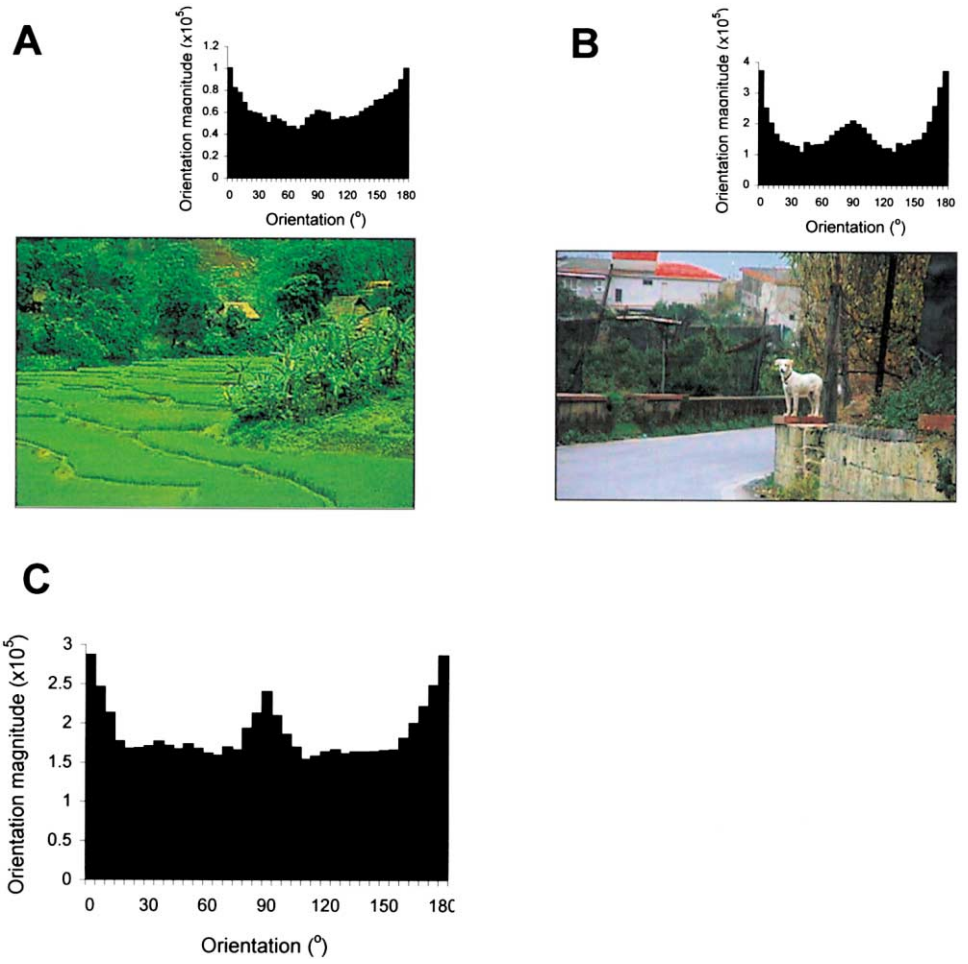

Figure 1. Analysis of Orientation Distribution of Natural Images

(A and B) Representative examples of natural scenes exhibiting overrepresentation of cardinal orientations. We have confirmed previous analyses reporting the overrepresentation of cardinal edges in natural scenes by calculating the orientation distribution of 32 natural images. We determined the orientation of each pixel based on the direction of the local grayscale gradient in a standard 9 pixel array from the arc tangent of the partial derivative of brightness in a 3 × 3 kernel in the vertical direction divided by this value in the horizontal direction. The orientation magnitude was calculated from the square root of the sums of the squares of the partial derivatives of brightness in the vertical and horizontal directions (the results were collapsed to a 0°–180° scale to generate orientation histograms for the full image). To validate this technique, we performed three control experiments. (1) We constructed an image patch comprised of random noise, in which case each orientation was equally represented in the scene. (2) A circular patch subtending the rectangular image was drawn (circle diameter was equal to the minimum of rectangle height and width), and the orientation distribution was calculated for the original patch and for the same patch tilted at 45°. In this case, the orientation distribution of the tilted patch was shifted by 45°. (3) We compared orientation histograms using a 3 × 3 pixel and a 5 × 5 pixel kernel size, but the results were not influenced by the scale of the analysis.

(C) Orientation histogram averaging 32 images which were randomly selected from a database containing digitized pictures of various natural environments.

V1 neuron is to adapt the cell to a stimulus of fixed orientation: such adaptation affects a broad range of orientations by selectively reducing responses near the adapting orientation (Blakemore et al., 1969; Movshon and Lennie, 1979; Saul and Cynader, 1989; Nelson, 1991; Carandini et al., 1998; Dragoi et al., 2000) and by inducing a shift in the neuron's preferred orientation away from the adapting stimulus (Müller et al., 1999; Dragoi et al., 2000). Given the narrower orientation distribution of local inputs to cardinal neurons compared to those of oblique neurons, an adapting stimulus (blue arrow, Figures 2C and 2D) oriented away from the neuron's preferred orientation (red arrow) would affect fewer neurons located within the local circuit of a cardinal cell compared to an oblique cell. Therefore, we hypothesized that altering the efficacy of local inputs through adaptation would induce larger changes in the orientation-specific responses of neurons tuned to oblique orientations compared to neurons tuned to cardinal orientations.

Results

To test this hypothesis, we measured the orientation tuning of V1 neurons before and after adaptation to a grating stimulus of fixed orientation. Even brief periods of adaptation cause systematic changes in orientation responses (Dragoi et al., 1999; Müller et al., 1999). Here,

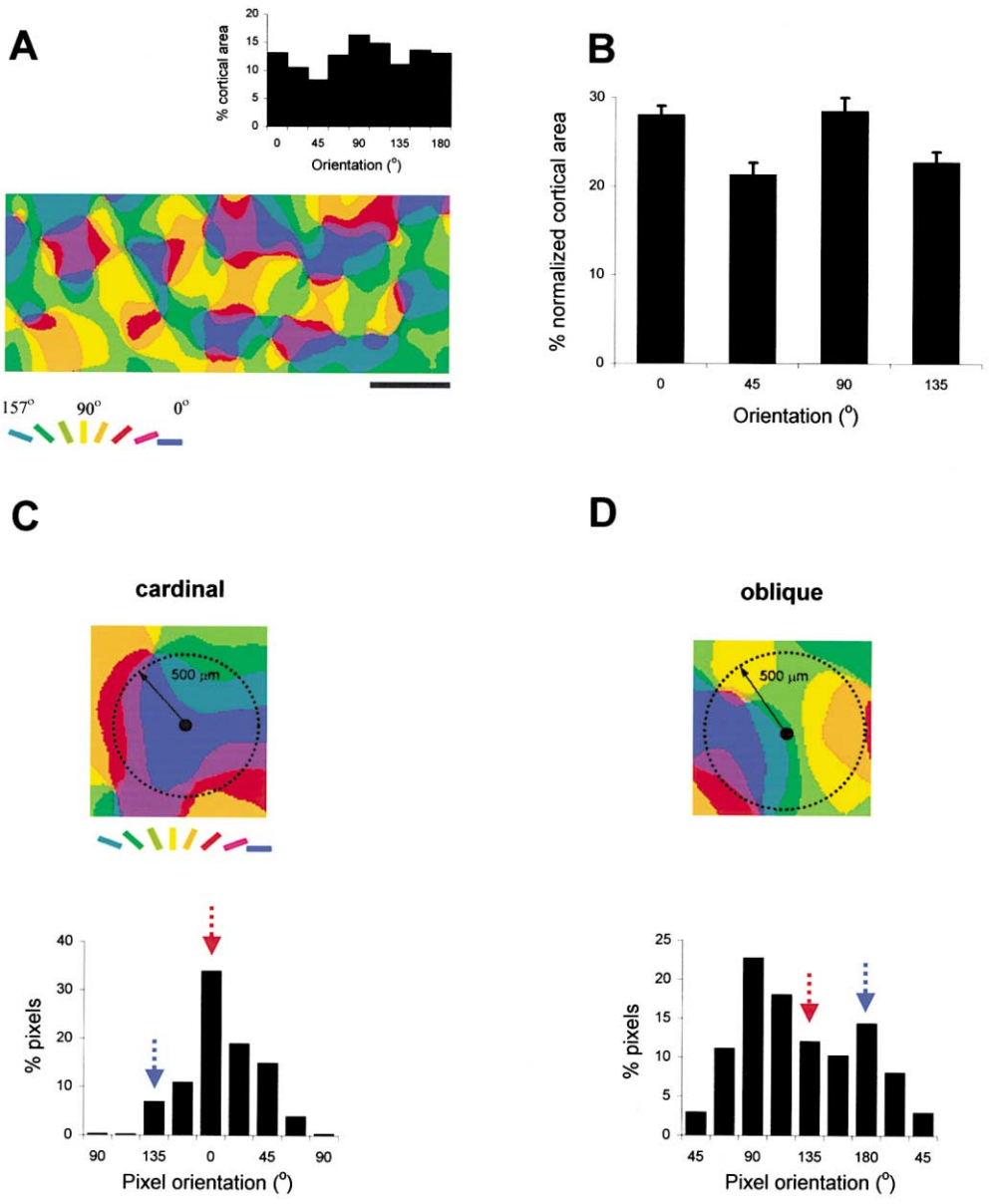

Figure 2. Overrepresentation of Horizontal and Vertical Orientations in V1 Maps

(A) Orientation distribution of pixels in one representative orientation preference map in adult cat V1. The area occupied by each orientation domain was calculated from the composite maps by counting the pixels responding best to different stimulus orientations (color key is shown on the bottom; bar length is 1 mm).

(B) Percent normalized cortical area responding best to cardinal (0° and 90°) and oblique (45° and 135°) orientations, after extracting the two cardinal and two oblique orientation domain areas from a set of eight orientations used to generate the orientation preference maps. The histogram was obtained after averaging data from 20 animals imaged as part of this and other experiments. Error bars represent the standard error of means. The overrepresentation of cardinal orientations is significant ($p < 0.002$, Student's t test).

(C and D) The local orientation distribution at different locations in the map of orientation preference.

(C) Orientation distribution of a circular area (500 μm radius) centered in the middle of a cardinal orientation domain. The dotted circle represents the pool of short-range intracortical inputs to the neuron marked by the small filled circle. The histogram represents pixel orientation distribution within the circular region.

(D) Orientation distribution of a circular area (500 μm radius) centered in the middle of an oblique orientation domain. In contrast to cardinal domains, neurons in the oblique domains receive broadly tuned oriented inputs. Presentation of an adapting stimulus potentially influences local intracortical inputs to cardinal neurons much less than it influences oblique neurons. The arrows indicate that adapting the neuron located in the middle of a cardinal orientation domain [red arrow in (C)] with a stimulus oriented 45° away from the neuron's preferred orientation ($\Delta\theta = 45°$, blue arrow) affects few inputs, whereas adapting the neuron located in the middle of an oblique orientation domain (red arrow in C) at the same $\Delta\theta = 45°$ affects many more inputs.

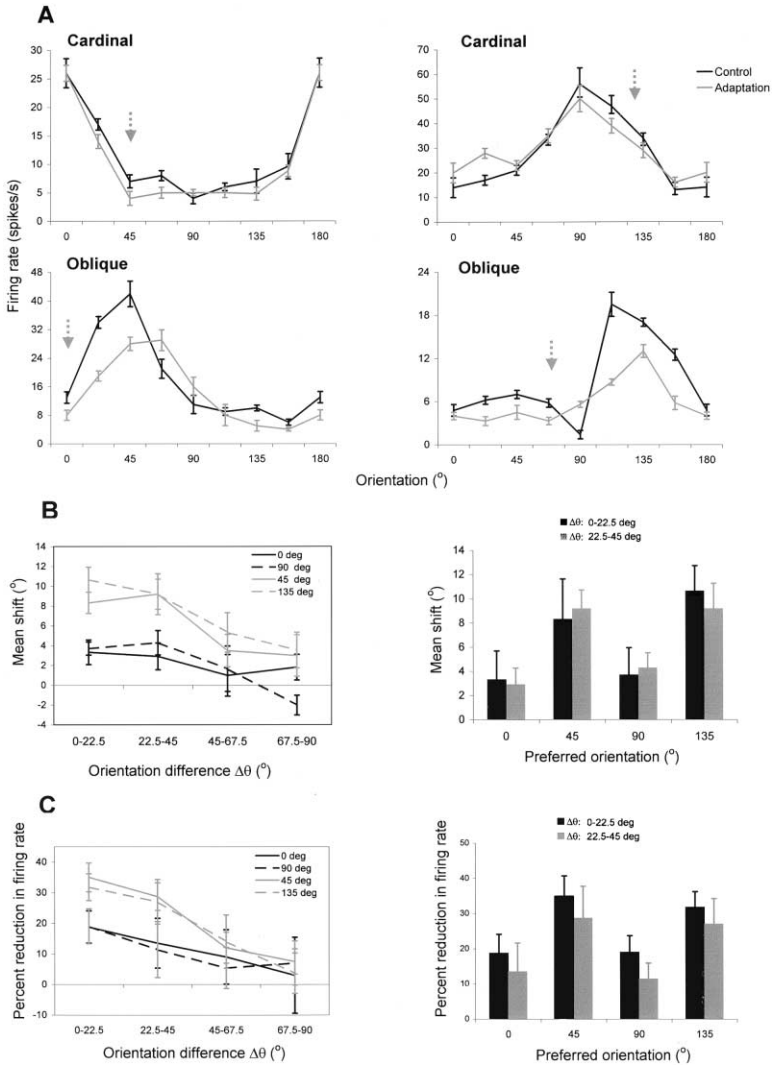

Figure 3. Meridional Asymmetry of Adaptation Effects

(A) Orientation tuning curves of four representative cardinal and oblique neurons during control (black) and adaptation (gray) conditions. The adapting orientation is marked by the gray arrow. The graphs represent mean values ± SEM.

(B) Changes in preferred orientation after short-term adaptation (n = 98 neurons). The left panel shows four curves derived by pooling the entire population of cells into four subpopulations of 0° (0° ± 15°, black), 90° (90° ± 15°, black dashed line), 45° (45° ± 30°, gray), and 135° (135° ± 30°, gray dashed line) after adaptation at a range of Δθs. Each point represents mean values ± SEM. The right panel is a histogram showing the changes in preferred orientation for the cardinal and oblique populations for the 0°–45° Δθ range.

(C) Changes in response at the control-preferred orientation after short-term adaptation. The left panel shows four curves derived by pooling the entire population of cells into two cardinal and two oblique populations similar to (B) (n = 98 neurons). For each cell we calculated the percent change in firing rate by comparing responses at the preadaptation preferred orientation during control and adaptation conditions, after subtraction of the d.c. component. The right panel is a histogram showing the changes in response at the control preferred orientation for the cardinal and oblique populations for the 0°–45° Δθ range.

we examined effects after relatively short (5 s) periods of adaptation. Figure 3A shows the tuning curves of representative neurons that demonstrate the meridional difference in changes induced by short-term adaptation. Depending on each cell's optimal orientation, the population of neurons was divided into four subpopulations: "horizontal" population, 0° ± 15°; "vertical" population, 90° ± 15°; and two "oblique" populations, 45° ± 30° and 135° ± 30°. After exposure to one orientation tilted with respect to each cell's preferred orientation by ~45°, the tuning curve profiles of cardinal and oblique neurons exhibit changes to different extents. Thus, whereas adaptation induces in each cell a repulsive shift in optimal orientation away from the adapting stimulus and a reduction of responses near the adapting orientation, large changes are observed only for the neurons tuned to oblique orientations. In contrast, neurons tuned to cardinal orientations exhibit much smaller changes in preferred orientation and firing rate. To characterize the meridional asymmetry of orientation adaptation, we determined quantitatively the relationship between Δθ (the difference between a neuron's optimal orientation and that of the adapting stimulus) and changes in orientation tuning for the entire population of cells (n = 98). For each cell, we evaluated whether a shift in preferred orientation was significant ($p < 0.05$, Student's t test) based on a trial-by-trial comparison between control and adaptation conditions. We found that although the cardinal and oblique neuronal populations do not differ in terms of their strength of orientation tuning ($p > 0.05$, Student's t test, comparing the orientation selectivity index of neurons in the two populations), short-term adaptation does induce asymmetric changes in preferred orientation and firing rate. Thus, for the Δθ range at which the adaptation effects are maximal, i.e., between 0° and 45°, 74% of the obliquely tuned neurons (21 of 28) showed significant shifts in orientation preference, compared to 23% of the neurons tuned to cardinal orientations (8 of 35). The mean shift magnitude histogram (Figure 3B, left), which was obtained by pooling each subpopulation into four Δθ bins, shows that the shift in optimal orientation is larger for the neurons tuned to oblique orientations for a broad range of Δθ values ($p < 0.05$, Student's t test, comparing changes in preferred orientation across oblique and cardinal subpopulations for the Δθ ranges of 0°–22.5° and 22.5°–45°).

In addition to the shift in orientation, adaptation reduces the response magnitude of V1 neurons. The reduction in firing rate, measured at the control optimal orientation, is also larger for the neurons tuned to the oblique orientations (Figure 3C, left) at a $\Delta\theta$ range between 0° and 45° ($p < 0.05$, Student's t test, comparing responses at the control preferred orientation for the oblique and cardinal subpopulations). For the same $\Delta\theta$ range, 80% of the obliquely tuned neurons (23 of 28) showed significant reductions in response at the control-preferred orientation, compared to 28% of the neurons tuned to cardinal orientations (10 of 35). At $\Delta\theta >$ 45°, the changes in preferred orientation and the depression in firing rate become smaller and the meridional asymmetry of adaptation is not statistically significant ($p > 0.05$, Student's t test).

To test the generality of the meridional asymmetry of adaptation, we exposed V1 neurons to a longer duration of the adapting stimulus (2 min), at which V1 neurons exhibit stronger adaptation effects (Dragoi et al., 2000). We investigated the changes in the orientation selectivity of 71 neurons after adaptation within the $\Delta\theta$ range of 0°–45°. In this case, we found that although 2 min of adaptation yields larger shifts in orientation preference and larger reductions in neuronal responses compared to 5 s of adaptation, the physiological difference between the cardinal and oblique populations remains intact. Thus, 80% of the obliquely tuned neurons (25 of 31) showed significant shifts in orientation preference compared to 35% of the neurons tuned to cardinal orientations (14 of 40), and 77% of the obliquely tuned neurons (24 of 31) showed significant reductions in the response at the control-preferred orientation compared to 27% of the neurons tuned to cardinal orientations (11 of 40).

It could be argued that the magnitude of changes in response properties shown in Figures 3B and 3C (right) is larger than that predicted by the difference between the size of cardinal and oblique domains (Figures 2A and 2B). However, since optical-imaging signals are mainly derived from the superficial layers, the magnitude of the cardinal overrepresentation over the entire V1 may be actually larger. The meridional asymmetry reported previously (Pettigrew et al., 1968; Blakemore and Cooper, 1970; Albus, 1975; Leventhal and Hirsch, 1977; Stryker et al., 1978; Kennedy and Orban, 1979) is stronger in simple cells and in the central visual field. Since there are few simple cells in the superficial layers of V1, and since our imaging areas often extend beyond the central visual representation, it is possible that our pixel analysis (Figures 2A and 2B) might have produced an underestimation of the anisotropy of cortical representation of different orientations. It is also possible that the larger changes in orientation tuning observed in cardinal neurons are due to different response properties of these neurons compared to those of the oblique cells. For instance, higher firing rates or narrower tuning bandwidths of cardinal neurons could possibly cause larger shifts in orientation tuning. In order to examine the relationship between the neuron's orientation preference and (1) the preadaptation peak firing rate and (2) the orientation tuning width, we recorded from 248 V1 neurons of various laminar location and found that the peak response at the optimal orientation and the orientation tuning width (Table 1), estimated calculating the orientation selectivity index, do not differ between the populations of cardinal and oblique neurons ($p > 0.05$, Student's t test, for OSI and firing rate comparisons between each pair of cardinal and oblique cell populations).

Table 1. OSI and Firing Rate Statistics for Different Classes of Cells

	OSI (Mean ± SEM)	Peak Firing Rate (Mean ± SEM)
Population	0.308 ± 0.011	23.98 ± 1.087
0° ± 15°	0.328 ± 0.025	26.41 ± 2.71
45° ± 30°	0.312 ± 0.018	24.27 ± 2.27
90° ± 15°	0.301 ± 0.024	23.22 ± 2.07
135° ± 30°	0.298 ± 0.021	22.87 ± 1.89

The mean and standard error of means for the orientation selectivity index (OSI) and peak firing rate for the total population of 248 neurons as well as for each class of cell (cardinal neurons, orientation preference range 0° ± 15° and 90° ± 15°, and oblique neurons, orientation preference range 45° ± 30° and 135° ± 30°).

The data presented in Figure 3 is consistent with our initial hypothesis that adaptation effects would be predicted from the local orientation distribution within an area surrounding the recording site. However, the data do not demonstrate that the orientation distribution in the local neighborhood of a neuron correlates with the changes in orientation-specific responses after adaptation. Indeed, since the cells that were analyzed in Figure 3 have not been localized within the orientation preference map, it is, in principle, possible that the larger adaptation effects exhibited by oblique neurons could be due to their proximity to orientation singularities (e.g., pinwheel centers) or to the feedforward influence exterted by cortical inputs from deeper layers of V1 or from LGN, independent on the orientation structure of the local intracortical circuit. For instance, we have shown previously (Dragoi et al., 2001) that neurons at or near regions of high local orientation gradient such as pinwheel centers are particularly susceptible to orientation plasticity induced by adaptation. Therefore, it could be possible that our sample of recording sites contains oblique sites that are closer (on average) to pinwheel centers; thus, they integrate inputs from neurons of broader orientation range.

To address the issue of cortical location, we used a combination of single-unit recording and optical imaging of intrinsic signals; the recordings were from cardinal and oblique neurons situated at different locations in the map of orientation preference, away from pinwheel centers. After intrinsic signals were imaged to obtain orientation preference maps in a patch of V1, we used the vascular pattern of the cortical surface in relation to the composite map to guide electrode penetrations aimed at cardinal or oblique iso-orientation domains (Figure 4A), recording at cortical depths between 300 and 800 μm. To understand the differences in the magnitude of changes induced by adaptation between cardinal and oblique neurons, we examined quantitatively the relationship between the local orientation distribution at the recording site and the degree of adaptation (Figure 4B). When the recording site is in the middle of a cardinal orientation domain, pixels within

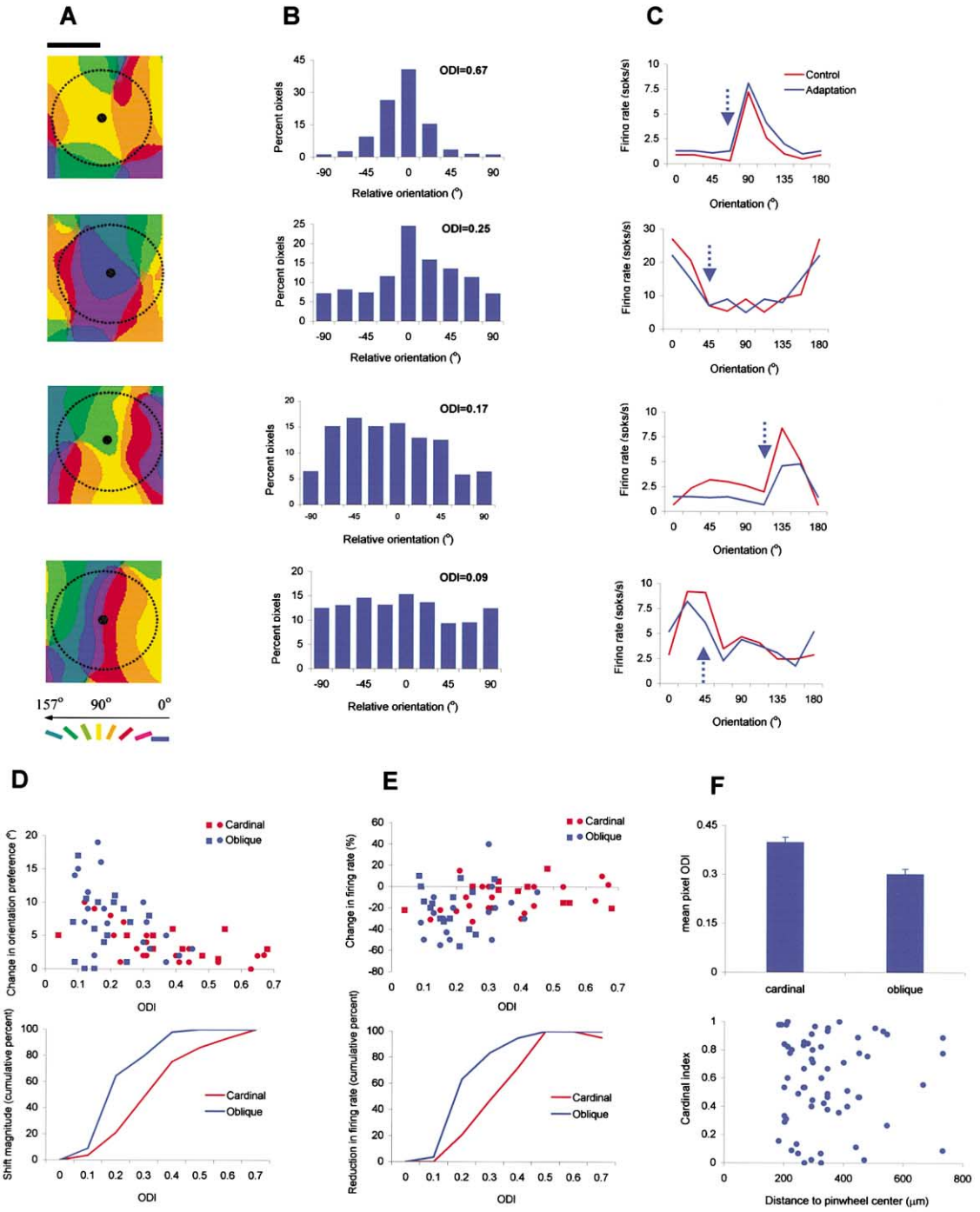

Figure 4. Relationship between the Local Orientation Distribution at the Recording Site and the Degree of Stability of Orientation Tuning

(A) Four recording sites placed respectively within iso-orientation cardinal domains (top two) and within iso-orientation oblique domains (bottom two). The recording sites are marked by small filled circles. The dotted circle of radius 500 μm represents the pixels within the local neighborhood of the recording site.

(B) The histograms of orientation distribution obtained after pooling the pixels into eight orientation bins between 0° and 180° (the +90° bin is repeated as the −90° bin). Each histogram is calculated from the corresponding composite map shown in (A). The orientation distribution index (ODI) represents a measure of the strength of orientation tuning for each histogram (see text).

(C) Orientation tuning curves during control (red) and after 2 min of adaptation (blue) for the cells recorded at the locations shown in (A). The adapting orientation is marked by the blue arrow.

(D) The top panel is a scatter plot (n = 65 cells) showing the magnitude of the postadaptation shift in preferred orientation (absolute values) for cardinal and oblique neurons as a function of the orientation distribution index (ODI) at the recording site. The bottom panel is a normalized cumulative histogram of the shift magnitude for the population of cardinal and oblique neurons as a function of the ODI range. Cardinal neurons are shown in blue, and oblique neurons are shown in red.

(E) The top panel is a scatter plot (n = 65 cells) showing the change in firing rate at the control preferred orientation for cardinal and oblique

a 500 μm radius have a preponderence of orientation preferences similar to the recorded neuron, whereas when the recording site is in the middle of an oblique domain, neighboring pixels have a larger orientation spread. We quantified the orientation spread of pixels within a local area (500 μm radius) by calculating an orientation distribution index (ODI), which is a measure of the pixel orientation tuning strength (similar to the orientation selectivity index). Interestingly, the higher the ODI at the recording site, the lower the magnitude of the shift in preferred orientation and the change in response magnitude. Figures 4B and 4C show representative examples that illustrate the dependence of adaptation-induced changes in orientation tuning on the orientation distribution of neighboring pixels. When the recording site is located in the middle of a cardinal orientation domain, the ODI is large and the changes in orientation selectivity induced by adaptation are minimal, whereas when the recording site is in the middle of an oblique orientation domain, the ODI is small and the orientation tuning curve undergoes pronounced changes.

Figures 4D and 4E characterize adaptation-induced changes in response properties in a population of 65 superficial-layer neurons of known map location. We found that since the cardinal orientation domains are (in general) larger than the oblique domains, cardinal neurons are likely to receive inputs from a narrower range of orientations than are oblique neurons (larger ODIs for the cardinal recording sites, $p < 0.0001$, Student's t test). Each neuron was adapted for 2 min to a grating of fixed orientation chosen to induce strong effects ($\Delta\theta < 45°$). For each neuron, we estimated the shift in preferred orientation and the change in firing rate at the control optimal orientation as a function of the ODI at the recording site. Figures 4D and 4E (top) show that there is a high inverse correlation between the orientation shift magnitude and the ODI (correlation coefficient $r = -0.59$, $p < 0.0001$, Pearson test) and a high correlation between the change in firing rate at the control orientation and the ODI (correlation coefficient $r = 0.33$, $p < 0.01$, Pearson test). Figures 4D and 4E (bottom) show that, after adaptation, the obliquely tuned neurons show both larger changes in orientation preference (mean shift 7.81 ± 0.84 versus 3.47 ± 0.46, $p < 0.0001$, Student's t test) and larger reductions in response magnitude (mean change in firing rate -21.5 ± 3.83 versus -9.93 ± 2.36, $p < 0.006$, Student's t test) compared to cardinal neurons. This demonstrates that the greater stability after adaptation is not due to a neuron's cardinal tuning per se, but due to the pooling of like orientations in large domains. Thus, adaptation induces changes in neuronal responses depending on the structure of the local neighborhood of each neuron: the broader the orientation distribution surrounding a V1 cell, the more pronounced the change in orientation tuning and firing rate.

To determine whether cardinal recording sites are indeed characterized by higher orientation distribution index values, we examined the relationship between each pixel's preferred orientation and the corresponding ODI for all the pixels in ten orientation maps obtained in the central visual field of V1 from ten animals. We pooled pixels based on their orientation preference in two groups, cardinal (0° and 90°) and oblique (45° and 135°), and found (Figure 4F, top) that the mean ODI of cardinal pixels is higher than the ODI of oblique pixels (0.398 ± 0.016 versus 0.301 ± 0.015, $p < 0.00004$, Student's t test).

As another test of whether the oblique neurons in our sample are situated closer to pinwheel centers, we examined whether the orientation preference at each recording site (represented by a cardinal index; see Experimental Procedures) varies with the distance to the nearest pinwheel center. However, we failed to find any correlation between the two (Figure 4F, bottom; correlation coefficient $r = -0.03$, $p > 0.2$, Pearson test), suggesting that our recordings were not biased by specific cortical location.

We next asked whether the meridional asymmetry of adaptation observed in V1 could give rise to similar anisotropies at the perceptual level. We thus examined the stability of tuning of human orientation detectors after short-term exposure to stimuli at a particular orientation. Short-term adaptation is a ubiquituous phenomenon in natural vision, and it is assumed to occur when series of nearby fixations to image patches correlated in orientation and spatial frequency are followed by eye movements to new spatial locations (Yarbus, 1967; Simoncelli and Schwartz, 1999). It is currently believed that such adaptation induces a shift in perceived orientation away from the adapting stimulus (the tilt aftereffect—Gibson and Radner, 1937; Ganz, 1966; Greenlee and Magnussen, 1987) that is equal in magnitude in both cardinal and oblique meridians (Mitchell and Muir, 1976). However, since Mitchell and Muir used relatively long adaptation periods (3 min) and long exposure intervals (2 s) for test gratings, it could, in principle, be possible that the tilt aftereffect exhibits a transient orientation asymmetry that could be revealed only by shorter stimulus durations. We thus tested the degree of stability of cardinal and oblique orientation detectors by measuring the perceived orientation of a sinusoidal high-contrast grating of orientation θ (target stimulus), which was briefly flashed for 50 ms before and after 1 s adaptation to a grating of orientation $\theta + 20°$ (Figure 5A; we determined that a 20° orientation difference between the target and adapting stimuli yields large shifts in perceived orientation). We collected data from five subjects who

neurons as a function of the orientation distribution index (ODI) at the recording site. The bottom panel is a normalized cumulative histogram of the change in firing rate for the population of cardinal and oblique neurons as a function of the ODI range. Cardinal neurons are shown in blue, and oblique neurons are shown in red. The data points marked by red and blue circles have been previously included in Figure 3 of Dragoi et al. (2001).

(F) The top panel is a histogram showing the mean ODI for cardinal and oblique pixels for all pixels in ten orientation maps. The error bars represent SEM. The bottom panel is a scatter plot ($n = 65$ cells) showing the cardinal index as a function of each cell's distance to the nearest pinwheel center.

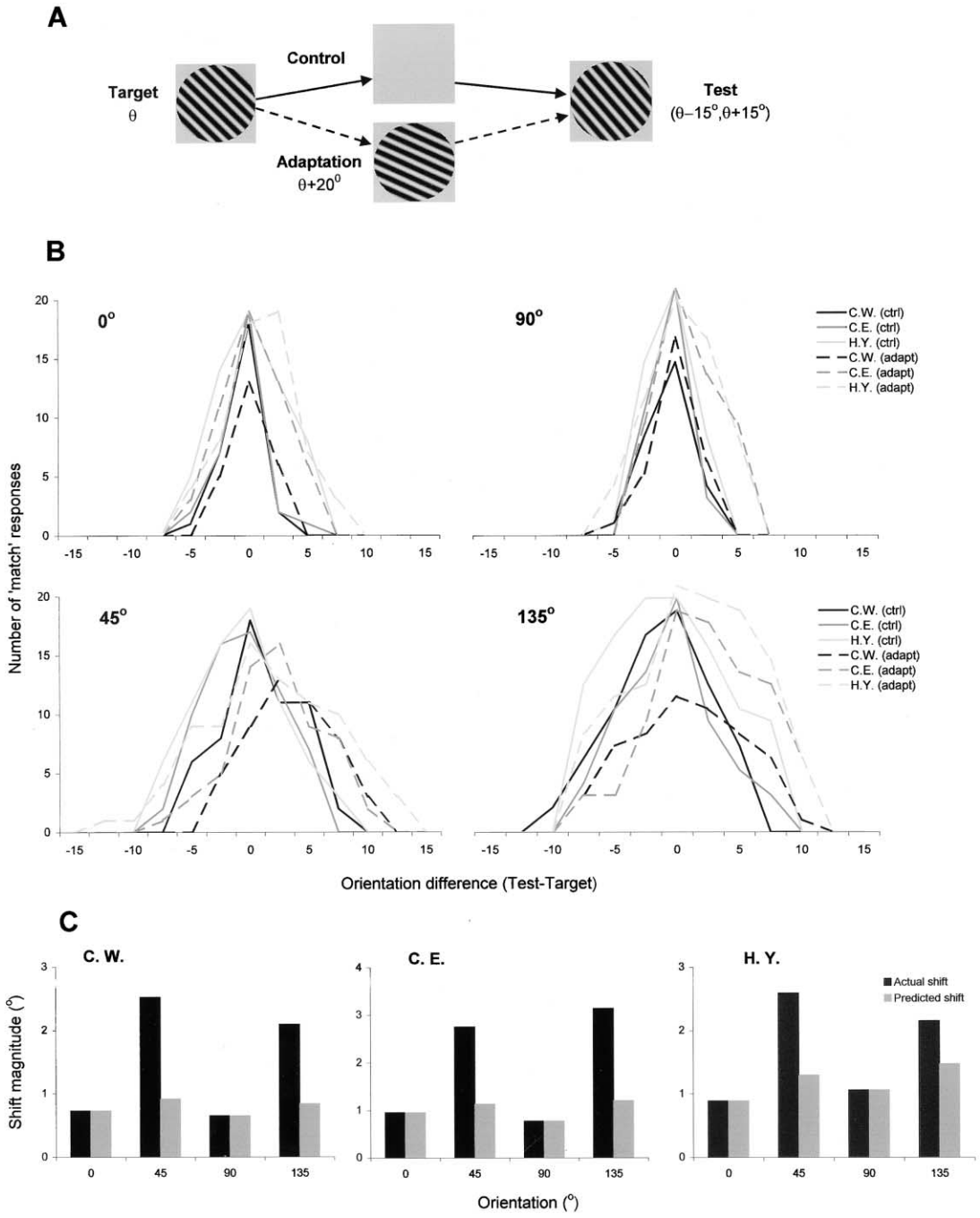

Figure 5. Anisotropy in Orientation Shifts of Human Observers after Short-Term Adaptation

(A) Subjects were required to respond when the orientation of a test stimulus matched that of the target. The target orientation was fixed at $\theta = 0°$, 45°, 90°, or 135°, while the test orientation varied in the range $\theta \pm 15°$ in orientation steps of 2.5°. Orientation tuning curves were calculated for all four target orientations after 1 s adaptation to a blank stimulus (control) or to a grating of orientation $\theta + 20°$ (adaptation).

(B) Psychophysical data from three naive subjects (C.W., black; C.E., dark gray; and H.Y., light gray). Tuning curves are plotted during control (solid lines) and adaptation (dashed lines) conditions for all four cardinal/oblique target orientations. The *y* axis represents the number of responses for each test orientation when subjects judged that the test orientation matched that of the target ("match" responses). The *x* axis represents the difference between test and target orientations.

(C) Histograms showing the magnitude of the repulsive shifts in preferred orientation (actual shift, black bars) separately for each subject and each target orientation. The predicted shifts in preferred orientation along the two oblique axes are represented by the gray bars. In calculating the predicted shifts (see text), we took the maximum predicted value from the two cardinal orientations.

viewed gratings at cardinal ($\theta = 0°$ and $\theta = 90°$) and oblique ($\theta = 45°$ and $\theta = 135°$) orientations presented foveally. We calculated how often the subjects reported that the target orientation matched that of a test grating (orientation range $\theta \pm 15°$) presented 100 ms after the offset of the adapting stimulus.

Figure 5B shows that adaptation induces repulsive changes in orientation tuning which are asymmetric with respect to the orientation axes. This figure presents data from three subjects who were naive to the purpose of the experiment. Thus, when orientation tuning curves were measured relative to the control condition, all subjects reported shifts in the orientation preference for the oblique gratings that were at least three times larger than the shifts for cardinal orientations. It is possible that the larger changes observed at oblique orientations are a consequence of the difference in the strength of tuning between cardinal and oblique orientation detectors (the oblique effect), and thus the perceptual orientation anisotropy reported here would be due to enhanced orientation discrimination along cardinal axes rather than being a direct effect of the meridional asymmetry of adaptation. If this hypothesis is correct, then compensating for the difference in the strength of orientation tuning between cardinal and oblique orientations should produce equal shifts in preferred orientation. We thus calculated a predicted shift for the oblique orientations as $shift_{obl} = shift_{card}\ (OSI_{obl})\ /\ (OSI_{card})$, where the subscripts *obl* and *card* denote oblique and cardinal orientations, and OSI (the orientation selectivity index) measures the strength of psychophysical orientation tuning. Figure 5C shows that the actual shifts obtained experimentally for oblique orientations are much larger than those predicted, thus suggesting that the meridional asymmetry of adaptation effects is not simply a consequence of the oblique effect but rather possibly reflects adaptation-induced orientation anisotropy similar to that found in V1 neurons.

Discussion

Our study suggests that the specific structure of orientation maps can influence cortical responses. The overrepresentation of cardinal versus oblique orientations in V1 maps limits short-term adaptation-induced plasticity of V1 neurons responsive to the cardinal versus oblique axes. This anisotropy, which is closely related to the local orientation distribution, can serve to impose stability on the processing of cardinal orientations during visual perception.

Linking the stability of cardinal orientations in human orientation detectors to the fact that cardinal neurons in V1 show stability after short-term adaptation requires the assumption that the activity across populations of V1 neurons is related to human observers' psychophysical performance. Similar assumptions have been previously made to explain enhanced performance on perceptual tasks such as orientation detection or discrimination along the cardinal axes (the oblique effect, e.g., Bauer et al., 1979; Boltz et al., 1979; Vandenbussche and Orban, 1980). Thus, it has been hypothesized (Kennedy and Orban, 1979) that small differences in the firing rates of single V1 neurons that are stimulated with different orientations could be enhanced by feedforward pooling and differentiation of signals from different cortical cells; larger responses across larger areas at cardinal orientations would underlie greater sensitivity to small changes. In addition, evoked-potential (Arakawa et al., 2000) and brain imaging studies (Furmanski and Engel, 2000) have reported an asymmetry in the magnitude of responses to oriented stimuli in V1 of humans that could possibly explain perceptual-orientation anisotropies. We propose that a larger cortical representation for cardinal orientations constrains the pooling and differentiation of neuronal signals from adjacent regions and thus underlies greater orientation stability along the cardinal axes during adaptation.

Our conclusions rely on the assumption that local intracortical connections are isotropic and that the connectivity rules are identical throughout the orientation map. Indeed, studies combining electrophysiological recordings and in vivo biocytin injections in cat areas 17 and 18 (Kisvarday et al., 1997) and intrinsic signal imaging and in vivo biocytin injections in monkey V1 (Malach et al., 1993) have reported that local intracortical connections are generally isotropic and are not orientation specific. In addition, crosscorrelation studies in cat V1 (Hata et al., 1991; Das and Gilbert, 1999) have revealed that the strength of local intracortical connections depends only on distance across the cortical surface and is independent of the relative orientation preference. It is also possible that the meridional anisotropy of adaptation is influenced by the network of long-range projections that reaches distances of up to a few millimeters in cortex (Gilbert and Wiesel, 1989; Bosking et al., 1997). Whereas local connections are less orientation specific and are denser close to the cell body, long-range connections, although sparser, tend to link domains sharing similar orientation preference (Ts'o et al., 1986; Malach et al., 1993). Thus, long-range interactions could enhance the effects of adaptation mediated primarily by local cortical networks.

A cardinal bias has been observed at subcortical sites of the adult visual pathway (e.g., the distribution of mammal retinal ganglion cells and their primary dendrites are more densely arrayed along the vertical and horizontal meridians; Wassle et al., 1975; Hughes, 1977; DeBruyn et al., 1980; Leventhal and Schall, 1983). However, because of the strong correlation between the clustered organization of orientation preference in the visual cortex and the degree of stability of orientation tuning (Figure 4), it would be difficult to argue that the asymmetry reported here originates in the retina or lateral geniculate nucleus. A related issue is whether the premise that the distribution of local inputs determines the asymmetry of adaptation can be reconciled with the fact that cardinal and oblique neurons have similar orientation tuning despite integrating differently tuned local intracortical inputs. We argue that it is possible that orientation adaptation would affect the strength of feedforward connections only weakly while inducing more pronounced changes in the strength of intracortical connections to produce changes in orientation selectivity after adaptation.

Adaptation to structural changes in the retinal image has been proposed to reduce the redundancy of natural signals in order to efficiently process visual information (Attneave, 1954; Barlow, 1990; Müller et al., 1999) by inducing changes in the neurons' firing rate (Movshon and Lennie, 1979; Ohzawa et al., 1982; Saul and Cynader, 1989; Carandini et al., 1998) and orientation tuning strength (Dragoi et al., 1999, 2000). However, in addition to these changes, adaptation has also been demon-

strated to induce transient shifts in the preferred orientation of V1 neurons (Dragoi et al., 2000) that could lead to a reorganization in the layout of cortical networks (Dragoi et al., 2000). This reorganization supports the idea of a continuous recalibration of the visual system in order to match changes in image structure (Andrews, 1964; Wolfe and O'Connell, 1986). How could the visual cortex prevent a global shift in the response properties of neurons while maintaining the beneficial effects of adaptation on information processing? While our study cannot fully answer this question, we propose that greater adaptation at oblique orientations would serve to increase information transfer at these orientations to compensate for reduced cortical representational size. At the same time, the greater tuning stability of cardinal neurons would limit the recalibration of the visual system along the cardinal axes. That is, one possible strategy of the visual system to minimize changes in perception due to cortical adaptation or plasticity could be to create a stable retinotopic frame of reference by retaining invariant cortical response properties along cardinal axes.

Experimental Procedures

Animals

Nine adult cats were used in these experiments. Animals were prepared for acute experiments according to protocols that were approved by MIT's Animal Care and Use Committee and conformed to NIH guidelines (Dragoi et al., 2000). Anesthesia was induced with ketamine (15 mg/kg, intramuscular [im]) and xylazine (1.5 mg/kg, im) and maintained with isofluorane (typically 0.5% to 1.5% in 70/30 mixture of N_2O/O_2) delivered through a tracheal cannula. Cats were paralyzed with intravenous norcuron (2.2 mg/kg) and artificially respired to maintain end-tidal CO_2 at approximately 4% at a partial pressure of 30 $\pm$ 3 mm Hg. Craniotomy followed by durotomy was performed to expose V1. Contact lenses were used to focus the eyes on a computer monitor and the location of the optic disks was plotted after the two retinas were backprojected on a screen situated 30 cm in front of the animal using a fiberoptic light guide. The position of the optic disks was used to align the two eyes along the horizontal axis and then infer the spatial location of the area centralis as 14.6° temporal and 6.5° inferior (Bishop et al., 1962).

Electrophysiology

Single-unit extracellular recordings were made using tungsten microelectrodes (1.5–2 MΩ resistance) which were advanced through the cortex using a pulse motor microdrive (Narishige Scientific Instruments Lab). The signal was amplified using an 8 channel differential amplifier (DataWave Technologies), thresholded using an amplitude discriminator, displayed on an oscilloscope (Tektronix TDS 210), and played over an audio monitor (Optimus). To ensure stable recordings, individual cells were isolated using a spike sort module (DataWave Technologies, v. 5.0) that allowed the identification and discrimination of waveforms based on their individual characteristics. The module consists of sorting the waveforms into separate clusters, analyzing individual clusters, and replaying the separated waveforms according to their cluster number. Waveform discrimination was based on extracting up to eight different waveform parameters, e.g., spike amplitude, spike width, peak time, and valley amplitude (allowing a maximum of 64 different combinations of waveform parameters). We also ensured that the minimum spike height was at least three times the largest noise signal in each recording. We recorded only single cells that had a minimum refractory period of 2 ms (determined using autocorrelation analysis). We recorded at cortical depths between 300 and 1500 μm from cells with initial orientation preferences covering the entire orientation range (between 0° and 180°). Stimuli consisted of 16 drifting high-contrast square-wave gratings, presented at orientations 22.5° apart at two directions of movement (opposite directions orthogonal to stimulus orientation). Typical stimulus parameters for V1 were spatial frequency 0.5 cycle/deg, temporal frequency 1 Hz. All stimuli were randomly interleaved. Stimuli were presented binocularly and were shown to the animal on a 17 inch monitor positioned 30 cm in front of it. We recorded responses during three conditions: before adaptation (control), when 16 drifting gratings were presented for ten trials each for a total of 160 trials, 2.5 s each presentation; during adaptation, when each grating was preceded by a 5 s presentation of an adapting grating of fixed orientation; and during recovery, when the 16 gratings were presented in identical conditions as in the control condition. The full protocol, including control, adaptation, and recovery periods, lasted about 1.5 hr.

The preferred orientation was calculated as described previously (Wörgötter and Eysel, 1991). The Fourier components were extracted from the orientation tuning curve and then normalized by dividing by the mean firing rate of the cell during stimulus presentation: $a = \sum_{i=0}^{N-1} R(\theta_i) cos(2\theta_i)$; $b = \sum_{i=0}^{N-1} R(\theta_i) sin(2\theta_i)$, where responses $R(\theta_i)$ are obtained after subtracting the spontaneous firing rate for a set of $N = 8$ test orientations θ_i, i = 0, 1 . . . N−1, which are uniformly distributed over 0°−180°, after averaging responses to the opposite directions of movement. Preferred orientation, θ, was calculated as $\theta = 0.5 arctan(b/a)$ if $a > 0$ or $\theta = 90 + 0.5 arctan(b/a)$ if $a < 0$. If $a > 0$ and $b < 0$, $\theta = 180 + 0.5 arctan(b/a)$. For each cell we calculated the percent change in firing rate by comparing responses at the preadaptation-preferred orientation during control and adaptation conditions after subtraction of the d.c. component. The strength of orientation tuning was given by the orientation selectivity index, $OSI = c / (MeanFiring)$, where $c = \sqrt{a^2 + b^2}$, and *MeanFiring* is the mean response magnitude averaged over orientation (Wörgötter and Eysel, 1991). For each neuron we calculated a cardinal index, which is 1 for cells oriented at 0° or 90° and 0 if the cells' preferred orientation is 45° or 135°. The cardinal index is defined by $CI(\theta) = 1 - (\theta) / 45$ if $\theta < 45°$, and $CI(\theta) = 1 - |\theta - 90|/45$ if $\theta > 45°$, where θ is the cell's preferred orientation (PO) if $PO < 90°$ or $|PO - 90|$ if $PO > 90°$.

Optical Imaging

Techniques for intrinsic signal imaging were similar to those described previously (Dragoi et al., 2000; Grinvald et al., 1986; Rao et al., 1997). A stainless-steel recording chamber (18 mm diameter, centered at coordinate P5.0) was attached to the skull surrounding the craniotomy, filled with silicone oil, and then sealed with a quartz plate. A video camera (CCD-5024N Bishke, Japan, RS-170, >60 dB signal to noise ratio) consisting of a 655 $\times$ 480 array of pixels equipped with a tandem-lens macroscope was positioned over the cortex. This arrangement gave a magnification of 75 pixels/mm. Data were collected using an imaging system (Optical Imaging). The camera signal was amplified by a video enhancement amplifier; a baseline image was subtracted from each stimulus response image in analog form and then digitized by an 8 bit analog-to-digital converter (Matrox) installed on a computer. Light from a 100 W tungsten-halogen light source driven by a dc power supply (Kepco) was passed through a filter and used to illuminate the cortex. Initially, a reference map of blood vessel pattern at the surface of the cortex was obtained by using light at 550 $\pm$ 40 nm. The camera was then focused 400–500 μm below the surface of the cortex and data was collected using light at 610 nm. Frames were summed between 0.5 and 3.5 s after stimulus onset, corresponding to the time of maximum signal as determined previously (Grinvald et al., 1986). The orientation gradient map was obtained by applying a two-dimensional gradient operator to the orientation preference map. For each pixel, the spatial gradient was given by $\sqrt{dx^2 + dy^2}$, where $dx = |\theta_{x+1,y} - \theta_{x,y}|$ and $dy = |\theta_{x,y+1} - \theta_{x,y}|$ [$\theta_{x,y}$ is the preferred orientation of pixel (x,y) in the composite map]. Values of *dx* and *dy* greater than 90° were subtracted from 180°, such that the maximum difference in preferred orientation was 90°. We related the gradient value at the recording site to changes in the orientation tuning of neurons by calculating the local orientation gradient as the mean of gradient values in a 3 $\times$ 3 pixel array centered at the penetration location. The gradient values were normalized for analysis. Data were analyzed using in-house programs written in Matlab.

Stimuli for optical imaging experiments were identical to those used in the extracellular recording, i.e., eight orientations between 0° and 180° separated by 22.5° and two opposite directions of motion

for each orientation. Orientation maps were obtained by averaging the optical signal acquired during 72 trials in each condition (eight single orientation responses) and then dividing them by responses to the blank screen (Grinvald et al., 1986; Dragoi et al., 2000). To obtain orientation preference maps, we summed vectorially the response at each pixel to the eight single stimulus orientations (including both directions of motion) and displayed the resultant angle of preferred orientation in pseudocolor form. Each map was smoothed using a low-pass filter, 5×5 kernel size, for display purposes (data analysis was performed on original, unfiltered, composite maps). In order to calculate the preferred orientation of individual pixels from eight single orientation responses, we used a method similar to that used for determining the preferred orientation of individual neurons (Wörgötter and Eysel, 1991; see above). For each recording site we determined an orientation distribution index (ODI) that measures the tuning strength of pixel orientation distribution in the local area surrounding the recording site. After pooling pixels within a local area (radius 500 μm) centered at the recording site into eight orientation bins separated by 22.5°, we calculated the ODI by applying the same method as for the OSI calculation. Fourier components were extracted from the pixel histogram $a = \Sigma_{i=0}^{N-1} P(\theta_i) cos(2\theta_i)$; $b = \Sigma_{i=0}^{N-1} P(\theta_i) sin(2\theta_i)$, where $P(\theta_i)$ represents the percentage of pixels of orientation θ_i, $i = 1, 2 \ldots 8$, which are uniformly distributed over 0°–157.5°. The orientation distribution index was given by $ODI = \sqrt{a^2 + b^2}$ (Wörgötter and Eysel, 1991; Dragoi et al., 2001).

Psychophysics

Stimuli were presented binocularly on a computer screen at a viewing distance of 60 cm and consisted of high-contrast (75%) 2.2 cpd sinusoidal circular gratings (5° in diameter) presented in the center of fixation (a fixation point of size 0.1° and 100% contrast always remained on the center of the screen). Each trial consisted of a 1800 ms cycle. The target was flashed for 50 ms at one of the following orientations ($\theta = 0°$, 45°, 90°, or 135°), followed after 100 ms by an adapting stimulus flashed for 1 s. The adapting stimulus consisted of a blank screen (uniform gray, 35 cd m^{-2}) or a sinusoidal grating (75% contrast, orientation $\theta + 20°$). Following a brief delay of 100 ms after the offset of the adapting stimulus, a test grating (75% contrast, orientation range $\theta \pm 15°$, random presentations at 2.5° orientation resolution) was briefly flashed for 50 ms. At the end of this presentation, subjects were asked to press a button within a 500 ms interval whenever the test orientation matched that of the target. The next trial started after an intertrial interval of 1 s (one session contained ~300 trials). Data collection took place only after the completion of a 10 day practice period, at the end of which each subject's performance reached stable performance levels. After calculating orientation tuning curves during both control and adaptation conditions, the changes in preferred orientation and the strength of tuning (OSI) were determined using the same method as that used for V1 neurons. Since the target and test stimuli were flashed only for a brief interval (50 ms), it is unlikely that subjects could use external cues, such as room and monitor edges, to estimate whether target and test orientations match. However, to control for this possibility, we collected additional data from two subjects (C.W. and one of the authors) in which a circular masking stimulus with a circular aperture in the center of fixation was used to occlude the monitor borders. The results of these control experiments were similar to those obtained without the use of a mask, i.e., at cardinal orientations the tilt aftereffect is much smaller compared to that found at oblique orientations (Figure 5).

Acknowledgments

We thank our subjects for participating in the experiment and Barton Anderson, Maximilian Riesenhuber, Casto Rivadulla, and Pawan Sinha for critical discussions. This work was supported by McDonnell-Pew and Merck fellowships to V.D. and by National Institutes of Health grant EY07023 to M.S.

Received April 13, 2001; revised November 7, 2001.

References

Albus, K. (1975). A quantitative study of the projection area of the central and the paracentral visual field in area 17 of the cat. II. The spatial organization of the orientation domain. Exp. Brain Res. *24*, 181–202.

Andrews, D.P. (1967). Perception of contour orientation in the central fovea. Part I: short lines. Vision Res. *7*, 975–997.

Arakawa, K., Tobimatsu, S., Kurita-Tashima, S., Nakayama, M., Kira, J.I., and Kato, M. (2000). Effects of stimulus orientation on spatial frequency function of the visual evoked potential. Exp. Brain Res. *131*, 121–125.

Attneave, F. (1954). Informational aspects of visual processing. Psychol. Rev. *61*, 183-193.

Barlow, H.B. (1990). A theory about the functional role and synaptic mechanism of after-effects. In Vision: Coding and Efficiency, C. Blakemore, ed. (Cambridge, UK: Cambridge Univeristy Press), p. 363-375.

Bauer, J.A., Jr., Owens, D.A., Thomas, J., and Held, R. (1979). Monkeys show an oblique effect. Perception *8*, 247–253.

Bishop, P.O., Kozak, W., and Vakkur, G.J. (1962). Some quantitative aspects of the cat's eye: axis and plane of references, visual field co-ordinates and optics. J. Physiol. *163*, 466–502.

Blakemore, C., and Campbell, F.W.J. (1969). Adaptation to spatial stimuli. J. Physiol. *200*, 11P–13P.

Blakemore, C., and Cooper, G.F.D. (1970). Development of the brain depends on the visual environment. Nature *228*, 477–478.

Blakemore, C., and Van Sluyters, R.C. (1975). Innate and environmental factors in the development of the kitten's visual cortex. J. Physiol. *248*, 663–716.

Blasdel, G.G. (1992). Differential imaging of ocular dominance and orientation selectivity in monkey striate cortex. J. Neurosci. *12*, 3115–3138.

Boltz, R.L., Harwerth, R.S., and Smith, E.L., III (1979). Orientation anisotropy of visual stimuli in rhesus monkey: a behavior study. Science *205*, 511–513.

Bonhoeffer, T., and Grinvald, A. (1991). Iso-orientation domains in cat visual cortex are arranged in pinwheel-like patterns. Nature *353*, 429–431.

Bosking, W.H., Zhang, Y., Schofield, B., and Fitzpatrick, D. (1997). Orientation selectivity and the arrangement of horizontal connections in tree shrew striate cortex. J. Neurosci. *15*, 2112–2127.

Campbell, F.W., Cleland, B.G., Cooper, G.F., and Enroth-Cugell, C. (1968). J. Physiol. *198*, 237–250.

Carandini, M., Movshon, J.A., and Ferster, D. (1998). Pattern adaptation and cross-orientation interactions in the primary visual cortex. Neuropharmacology *37*, 501–511.

Chapman, B., and Bonhoeffer, T. (1998). Overrepresentation of horizontal and vertical orientation preferences in developing ferret area 17. Proc. Natl. Acad. Sci. USA *95*, 2609–2614.

Coppola, D.M., Purves, H.R., McCoy, A.N., and Purves, D. (1998a). The distribution of oriented contours in the real world. Proc. Natl. Acad. Sci. USA *95*, 4002–4006.

Coppola, D.M., White, L.E., Fitzpatrick, D., and Purves, D. (1998b). Unequal representation of cardinal and oblique contours in ferret visual cortex. Proc. Natl. Acad. Sci. USA *95*, 2621–2623.

Coppola, D.M., Panos, V., and White L.E. (2000). Unequal representation of cardinal and oblique contours in ferret visual cortex: normal development and the effects of altered visual experience. Abstr. Soc. Neurosci. 26.

Das, A., and Gilbert, C.D. (1999). Topography of contextual modulations mediated by short-range interactions in primary visual cortex. Nature *399*, 655–661.

DeBruyn, E.J., Wise, V.L., and Casagrande, V.A. (1980). The size and topographic arrangement of retinal ganglion cells in the galago. Vision Res. *20*, 315–327.

De Valois, R.L., Yund, E.W., and Hepler, N. (1982). The orientation

and direction selectivity of cells in macaque visual cortex. Vision Res. *22*, 531–544.

Dragoi, V., Sharma, J., Miller, E.K.M., and Sur, M. (1999). Dynamics of orientation adaptation in awake monkey V1 revealed by reverse correlation. Abstr. Soc. Neurosci. *25*, 1548.

Dragoi, V., Sharma, J., and Sur, M. (2000). Adaptation-induced plasticity of orientation tuning in adult visual cortex. Neuron *28*, 287–298.

Dragoi, V., Rivadulla, C., and Sur M. (2001) Foci of orientation plasticity in visual cortex. Nature *411*, 80-86.

Durbin, R., and Mitchison, G. (1990). A dimension reduction framework for understanding cortical maps. Nature *343*, 644–647.

Furmanski, C.S., and Engel, S.A. (2000). An oblique effect in human primary visual cortex. Nat. Neurosci. *3*, 535–536.

Ganz, L. (1966). Mechanisms of figural after-effects. Psychol. Rev. *73*, 128–150.

Gibson, J.J., and Radner, M. (1937). Adaptation, after-effect and contrast in the perception of tilted lines. I Quantitative studies. J. Exp. Psychol. *20*, 453–467.

Gilbert, C.D., and Wiesel, T.N. (1989). Columnar specificity of intrinsic horizontal and corticocortical connections in cat visual cortex. J. Neurosci. *9*, 2432–2442.

Greenlee, M.W., and Magnussen, S. (1987). Saturation of the tilt aftereffect. Vision Res. *27*, 1041–1043.

Grinvald, A., Lieke, E., Frostig, R.D., Gilbert, C.D., and Wiesel, T.N. (1986). Functional architecture of cortex revealed by optical imaging of intrinsic signals. Nature *324*, 361–364.

Hata, Y., Tsumoto, T., Sato, H., and Tamura, H. (1991). Horizontal interactions between visual cortical neurones studied by cross-correlation analysis in the cat. J. Physiol. *441*, 593–614.

Hubel, D.H., and Wiesel, T.N. (1974). Sequence regularity and geometry of orientation columns in the monkey striate cortex. J. Comp. Neurol. *158*, 267–293.

Hübener, M., Shoham, D., Grinvald, A., and Bonhoeffer, T. (1997). Spatial relationships among three columnar systems in cat area 17. J. Neurosci. *17*, 1270–1284.

Hughes, A. (1977). In The Visual System in Vertebrates, F. Crescitelli, ed. (Heidelberg: Springer Verlager), pp. 613–756.

Kennedy, H., and Orban, G.A. (1979). Preferences for horizontal or vertical orientation in cat visual cortical neurones. J. Physiol. *296*, 61P–62P.

Kisvarday, Z.F., Toth, E., Rausch, M., and Eysel, U.T. (1997). Orientation-specific relationship between populations of excitatory and inhibitory lateral connections in the visual cortex of the cat. Cereb. Cortex *7*, 605–618.

Koulakov, A.A., and Chlovskii, D.B. (2001). Orientation preference patterns in mammalian visual cortex: a wire length minimization approach. Neuron *29*, 519-527.

Leventhal, A.G., and Hirsch, H.V. (1977). Effects of early experience upon orientation sensitivity and binocularity of neurons in visual cortex of cats. Proc. Natl. Acad. Sci. USA *74*, 1272–1276.

Leventhal, A.G., and Schall, J.D. (1983). Structural basis of orientation sensitivity of cat retinal ganglion cells. J. Comp. Neurol. *220*, 465–475.

Levitt, J.B., Kiper, D.C., and Movshon, J.A. (1994). Receptive fields and functional architecture of macaque V2. J. Neurophysiol. *71*, 2517–2542.

Malach, R., Amir, Y., and Grinvald, A. (1993). Relationship between intrinsic connections and functional architecture revealed by optical imaging and *vivo* tangential biocytin injections in primate striate cortex. Proc. Natl. Acad. Sci. USA *90*, 10469–10473.

Mitchell, D.E., and Muir, D.W. (1976). Does the tilt after-effect occur in the oblique meridian? Vision Res. *16*, 609–613.

Movshon, A., and Lennie, P. (1979). Pattern-selective adaptation in visual cortical neurones. Nature *278*, 850–852.

Müller, J.R., Metha, A.B., Krauskopf, J., and Lennie, P. (1999). Rapid adaptation in visual cortex to the structure of images. Science *285*, 1405–1408.

Müller, T., Stetter, M., Hübener, M., Sengpiel, F., Bonhoeffer, T., Godecke, I., Chapman, B., Lowel, S., and Obermayer, K. (2000). An analysis of orientation and ocular dominance patterns in the visual cortex of cats and ferrets. Neural Comput. *12*, 2573–2595.

Nelson, S.B. (1991). Temporal interactions in the cat visual system. I. Orientation-selective suppression in the visual cortex. J. Neurosci. *11*, 344–356.

Ohzawa, I., Sclar, G., and Freeman, R.D.S. (1982). Contrast gain control in the cat visual cortex. Nature *298*, 266–268.

Pettigrew, J.D., Nikara, T., and Bishop, P.O. (1968). Responses to moving slits by single units in cat striate cortex. Exp. Brain Res. *6*, 373–390.

Rao, S.C., Toth, L.J., and Sur, M. (1997). Optically imaged maps of orientation preference in primary visual cortex of cats and ferrets. J. Comp. Neurol. *387*, 358–370.

Rose, D., and Blakemore, C. (1974). An analysis of orientation selectivity in the cat's visual cortex. Exp. Brain Res. *20*, 1–47.

Saul, A.B., and Cynader, M.S. (1989). Adaptation in single units in visual cortex: the tuning of aftereffects in the spatial domain. Vis. Neurosci. *2*, 593–607.

Sengpiel, F., Stawinski, P., and Bonhoeffer, T. (1999). Influence of experience on orientation maps in cat visual cortex. Nat. Neurosci. *2*, 727–732.

Simoncelli, E.P., and Schwartz, O. (1999). Modeling surround suppression in V1 neurons with a statistically-derived normalization model. In Advances in Neural Information Processing Systems, Volume 11, M.S. Kearns, S.A. Solla, and D.A. Cohn, eds. (Cambridge, MA: MIT Press).

Stryker, M.P., Sherk, H., Leventhal, A.G., and Hirsch, H.V. (1978). Physiological consequences for the cat's visual cortex of effectively restricting early visual experience with oriented contours. J. Neurophysiol. *41*, 896–909.

Swindale, N.V., Shoham, D., Grinvald, A., Bonhoeffer, T., and Hübener, M. (2000). Visual cortex maps are optimized for uniform coverage. Nat. Neurosci. *3*, 822–826.

Switkes, E., Mayer, M.J., and Sloan, J.A. (1978). Spatial frequency analysis of the visual environment: anisotropy and the carpentered environment hypothesis. Vision Res. *18*, 1393–1399.

Ts'o D.Y., Gilbert C.D., and Wiesel, T.N. (1986). Relationships between horizontal interactions and functional architecture in cat striate cortex as revealed by cross-correlation analysis. J. Neurosci. *6*, 1160–1170.

Vandenbussche, E., and Orban, G.A. (1980). Differential orientation thresholds as a function of orientation in the cat. Arch. Int. Physiol. Biochim. *88*, P11–P12.

Wassle, H., Levick, W.R., and Cleland, B.G. (1975). The distribution of the alpha type of ganglion cells in the cat's retina. J. Comp. Neurol. *159*, 419–438.

Weliky, M., Kandler, K., Fitzpatrick, D., and Katz, L.C. (1995). Patterns of excitation and inhibition evoked by horizontal connections in visual cortex share a common relationship to orientation columns. Neuron *15*, 541–552.

Wolfe, J.M., and O'Connell, K.M. (1986). Fatigue and structural change: two consequences of visual pattern adaptation. Invest. Ophthalmol. Vis. Sci. *27*, 538–543.

Wörgötter, F., and Eysel, U.T. (1991). Correlations between directional and orientational tuning of cells in cat striate cortex. Exp. Brain Res. *83*, 665–669.

Yarbus, A.L. (1967). Eye Movement and Vision (New York: Plenum Press).